

# Porous silicon Bragg reflectors with sub-micrometer lateral dimensions

Mark B. H. Breese and Dharmalingam Mangaiyarkarasi

Centre for Ion Beam Applications, 2 Science Drive 3, Department of Physics,  
National University of Singapore, Singapore 117542

[phymbhb@nus.edu.sg](mailto:phymbhb@nus.edu.sg)

<http://www.ciba.nus.edu.sg>

**Abstract:** Bragg reflectors with widths down to 300 nm have been fabricated in porous silicon. This was achieved by irradiation of highly-doped *p*-type silicon with a focused beam of high-energy ions in a channeled alignment, in which the beam is aligned with a major crystallographic direction. The reflected colour is controllably tuned across the visible spectrum by varying the ion irradiated dose. The depth distribution of ion induced defects differs in channeled alignment compared to random beam alignment, resulting in the hole current during subsequent anodisation being more confined to narrower lateral regions, enabling different reflective wavelengths to be patterned on a sub-micron lateral scale. This work provides a means of producing high-density arrays of micron-size reflective colour pixels for uses in high-definition displays, and selectively tuning the wavelengths of porous silicon Fabry-Perot microcavities across the visible and infra-red ranges for optical communications and computing applications.

©2007 Optical Society of America

OCIS codes: (230.1480) Bragg reflectors; (230.4170) Multilayers; (130.0520) Optoelectronics.

## References and links

1. G. Vincent, "Optical properties of porous silicon superlattices," *Appl. Phys. Lett.* **64**, 2367-2369 (1994).
2. M. G. Berger, R. Arens-Fischer, M. Kruger, S. Billat, H. Luth, S. Hillbrich, W. Theiß, and P. Grosse, "Dielectric filters made of PS: advanced performance by oxidation and new layer structures," *Thin Solid Films* **297**, 237-240 (1997).
3. M. Araki, H. Koyama, and N. Koshida, "Controlled electroluminescence spectra of porous silicon diodes with a vertical optical cavity," *Appl. Phys. Lett.* **69**, 2956-2958 (1996).
4. L. Pavesi, "Porous silicon dielectric multilayers and microcavities," *Riv. Nuovo Cimento* **20**, 1-78 (1997).
5. S. Nagata, C. Domoto, T. Nishimura, and K. Iwameji, "Single-mode optical waveguide fabricated by oxidation of selectively doped titanium porous silicon," *Appl. Phys. Lett.* **72**, 2945-2947 (1998).
6. A. Birner, R. B. Wehrspohn, U. Gösele, and K. Busch, "Silicon-Based Photonic Crystals," *Adv. Mater.* **13**, 377-388 (2001).
7. N. Savage, "Linking with light," *IEEE Spectrum* **39**, 32-36 (2002).
8. V. Lehmann, *Electrochemistry of Silicon* (Wiley-VCH, Weinheim, Germany 2002).
9. D. Mangaiyarkarasi, M. B. H. Breese, Y. S. Ow, and C. Vijila, "Controlled blue-shift of the resonant wavelength in porous silicon microcavities using ion irradiation," *Appl. Phys. Lett.* **89** 021910-(1-3) (2006).
10. M. B. H. Breese, F. J. T. Champeaux, E. J. Teo, A. A. Bettiol, and D. Blackwood, "Hole transport through proton-irradiated *p*-type silicon wafers during electrochemical anodization," *Phys. Rev. B* **73** 035428(1-7) (2006).
11. D. S. Gemmell, "Channeling and related effects in the motion of charged particles through crystals" *Rev. Mod. Phys.* **46**, 129-227 (1974).
12. L. C. Feldman, J. W. Mayer, S. T. Picraux, *Materials Analysis by Ion Channeling* (Acad. Press, New York, 1982).
13. P. J. C. King, M. B. H. Breese, P. J. C. Smulders, P. R. Wilshaw and G. W. Grime, "The observation of a blocking to channeling transition for MeV protons at stacking faults in silicon. *Phys. Rev. Lett.* **74**, 411-414 (1995).
14. M. B. H. Breese, P. J. C. King, P. J. C. Smulders, and G. W. Grime, "Dechanneling of MeV protons by 60° dislocations" *Phys. Rev. B* **51**, 2742-2750 (1995).

15. M. B. H. Breese, D. N. Jamieson and P. J.C.King, *Materials Analysis using a Nuclear Microprobe*, (Wiley, New York, 1996).
  16. M. B. H. Breese, E. J. Teo, M. A. Rana, L. Huang, J. A. van Kan, F. Watt, and P. J. C. King, "Observation of many coherent oscillations for MeV protons transmitted through stacking faults," *Phys. Rev. Lett.* **92**, 045503 (2004).
  17. Ocean Optics <http://www.oceanoptics.com/products/colorfilters.asp>
- 

## 1. Introduction

One dimensional photonic structures based on alternating high and low porosity porous silicon layers have found applications in silicon photonics, such as dielectric mirrors in the form of Distributed Bragg Reflectors[1, 2], optical microcavities[3, 4], waveguides[5] and possibly as optical interconnects and switches[6, 7]. One dimensional porous silicon Bragg reflectors are easily produced by periodically raising and lowering the electrochemical hole current flowing through highly-doped *p*-type silicon during anodisation. The porosity, hence effective refractive index of each layer, is determined by the hole current density[4, 8]. When each alternating high/low refractive index porous layer has an optical thickness of one quarter of the wavelength of incident light this wavelength is constructively reflected with an efficiency approaching 100% for more than ten pairs of layers. Until recently there has been no means of fabricating highly-reflective arrays of colour filters on a micrometer lateral scale, so applications as high-density reflective displays and in photonics have not been possible.

## 2. Experiment

We recently showed [9] how the peak wavelength of light reflected and transmitted from porous silicon Bragg reflectors and optical microcavities may be controllably blue-shifted across the visible spectrum using ion irradiation, and 10  $\mu\text{m}$  reflective regions were produced. A focused 2 MeV proton beam was used to selectively irradiate a 0.02  $\Omega\cdot\text{cm}$  *p*-type wafer with doses up to  $2 \times 10^{15}/\text{cm}^2$  in a random alignment. Such irradiation damages the silicon lattice by producing defects which locally reduce the concentration of free charge carriers [10]. The increased resistivity leads to a reduction in the hole current passing through, and adjacent to, the irradiated regions during subsequent anodisation. This reduces the optical thickness of each anodized layer, resulting in a Bragg reflector in which the peak reflected wavelength is linearly blue-shifted with increasing irradiation dose, as shown in Fig. 1(a). The first data point of 740 nm corresponds to that measured from the unirradiated background. The ion irradiated silicon was anodized at room temperature in a solution of HF (48%): water: ethanol in the ratio of 1:1:2 to form twelve pairs of high/low refractive index layers. It was then washed in ethanol and dried in air. Figures 1(b) to 1(d) show reflective colour stripes and pixels with dimensions ranging from 10 to 2  $\mu\text{m}$  produced using this process, where the reflected colours are highly uniform due to improved uniformity of irradiation. Red/yellow/green/blue reflective colours are respectively produced by irradiation with 1 to 4 dose increments of  $4 \times 10^{14}/\text{cm}^2$ . The measured reflectivity of the 10  $\mu\text{m}$  and 2  $\mu\text{m}$  reflectors is typically 50% and 40% respectively across the visible spectrum.

Figure 2(a) shows a cross-section SEM of the 2  $\mu\text{m}$  wide irradiated lines in which a width of the transition region between two irradiated doses of  $\sim 1 \mu\text{m}$  is observed. Hence in Fig. 2(b), which shows linescans of the reflective colours measured across the 2  $\mu\text{m}$  wide pixels, only the central 1  $\mu\text{m}$  exhibits uniform reflection since the outer portions comprise part of the transition region to an adjacent line. Reference [10] gives computer simulations of the effect of ion irradiation in a random alignment on the hole current density flowing through and around adjacent areas during electrochemical anodisation. A transition width between two irradiations of  $\sim 1 \mu\text{m}$  was observed in these simulations, in agreement with Fig. 2. This paper demonstrates how this limitation to the formation of sub-micron reflective regions may be overcome by irradiation in a channeled alignment.

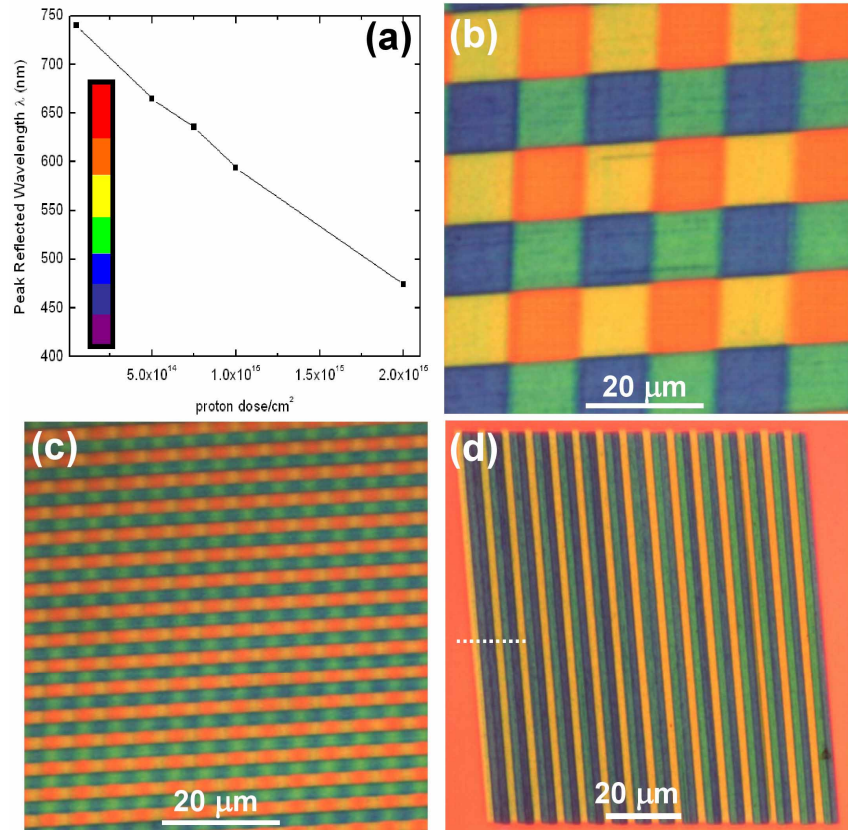


Fig. 1. (a). Peak reflected wavelength of porous silicon Bragg reflectors versus proton irradiation dose. The corresponding reflective colour is also shown. (b), (c), (d) respectively show optical images of the reflected light from  $60 \times 60 \mu\text{m}^2$  regions of porous silicon Bragg reflectors patterned with 10  $\mu\text{m}$  and 2  $\mu\text{m}$  wide colour pixels and 2  $\mu\text{m}$  wide colour stripes.

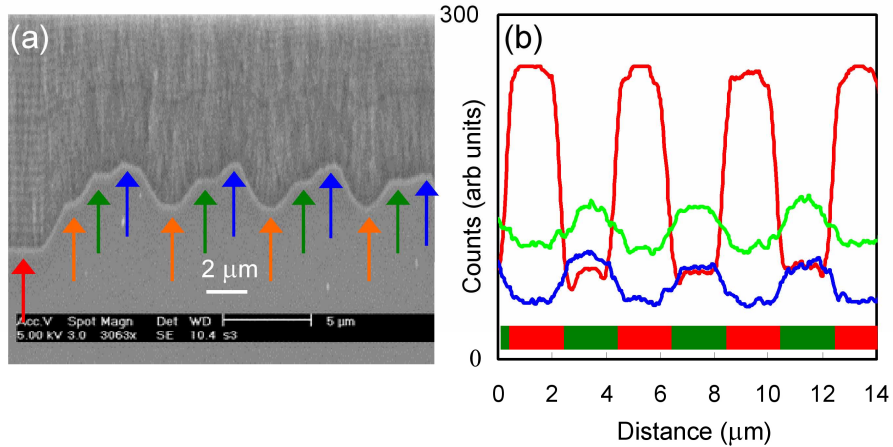


Fig. 2. (a). Cross-section SEM of the porous silicon Bragg reflector patterned with 2  $\mu\text{m}$  wide lines in Fig. 1(d), from the region indicated by the dashed white line, with the unirradiated red background at the left side. (b) Linescan of recorded reflected intensity for red, green, blue from the 2  $\mu\text{m}$  pixels in Fig. 1(c).

Positively-charged, high-energy ions undergo a channelling process when aligned with a crystal direction, in which they are repelled from the lattice plane walls into regions of lower electron density close to the channel centre [11, 12]. Channeled ions have a lower rate of electronic energy loss and a lower probability of scattering from lattice nuclei, so a lower rate of defect production compared to a randomly aligned beam. The planar channelling critical angle for 2 MeV protons, which is the maximum angle for which the silicon (110) lattice planes can maintain a channeled trajectory, is  $\Psi_p = 0.17^\circ$ ; for larger tilts the beam has a random trajectory. References [13, 14] describes the use of MeV protons focused using a nuclear microprobe [15] to produce spatially-resolved transmission channelling images of defects using this principle. A high-demagnification microprobe capable of focusing to a spot size of  $\sim 60$  nm [16] was used here to irradiate silicon in channeled alignment. Figure 3 shows the effect of a channeled beam irradiation with 1  $\mu\text{m}$  wide lines with doses corresponding to red-green-blue periodic reflective regions. Each 1  $\mu\text{m}$  wide irradiated line reflects two different colours in Fig. 3(a), resulting in a total of six colours reflected within each 3  $\mu\text{m}$  wide period.

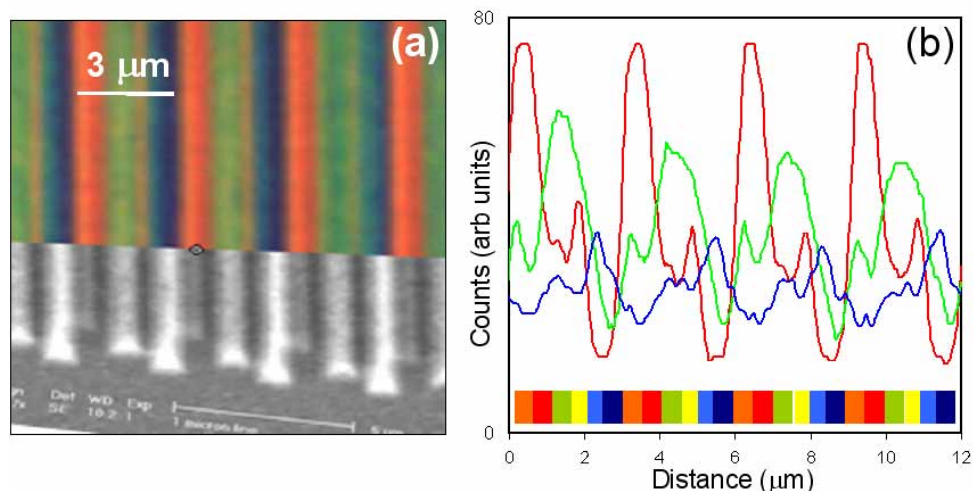


Fig. 3. (a). Optical image of the reflected light from a region of a porous silicon Bragg reflector formed by irradiation with 1  $\mu\text{m}$  wide lines in channeled alignment. A SEM image of the same region in which the porous silicon removed to show the surface profile is shown in the lower half. (b) Linescan of recorded reflected intensity for red, green, blue from the 1  $\mu\text{m}$  wide irradiated lines in Fig. 3(a).

The explanation how such narrow reflective colour lines can be fabricated using channeled beam irradiation is shown schematically in Fig. 4. In Fig. 4(a) adjacent regions are irradiated in both random and channeled alignment with two doses, e.g. those which produce green and blue reflective regions, with the lower dose to the left. In a random beam irradiation the defect profile comprises a uniform, low (grey) density region extending from the surface to a depth of 45  $\mu\text{m}$ , and a region of high defect density (black) around the end of range, from a depth of about 45 to 50  $\mu\text{m}$ . In Fig. 4(b) the hole current flowing through the wafer during anodisation is deflected away from the randomly irradiated region, reaching the surface at a distance up to several microns away, depending on the dose and wafer resistivity<sup>10</sup>. This results in a wide transition region of typically  $\sim 1$   $\mu\text{m}$  in Fig. 4(c) between the randomly irradiated regions. The thickness of the overlying Bragg reflecting porous silicon layers follows the same trend, producing the wide transition regions between the reflected green and red colours in Fig. 2. A

SEM of the resultant surface structure produced in random and channeled alignment is compared in Fig. 4(d).

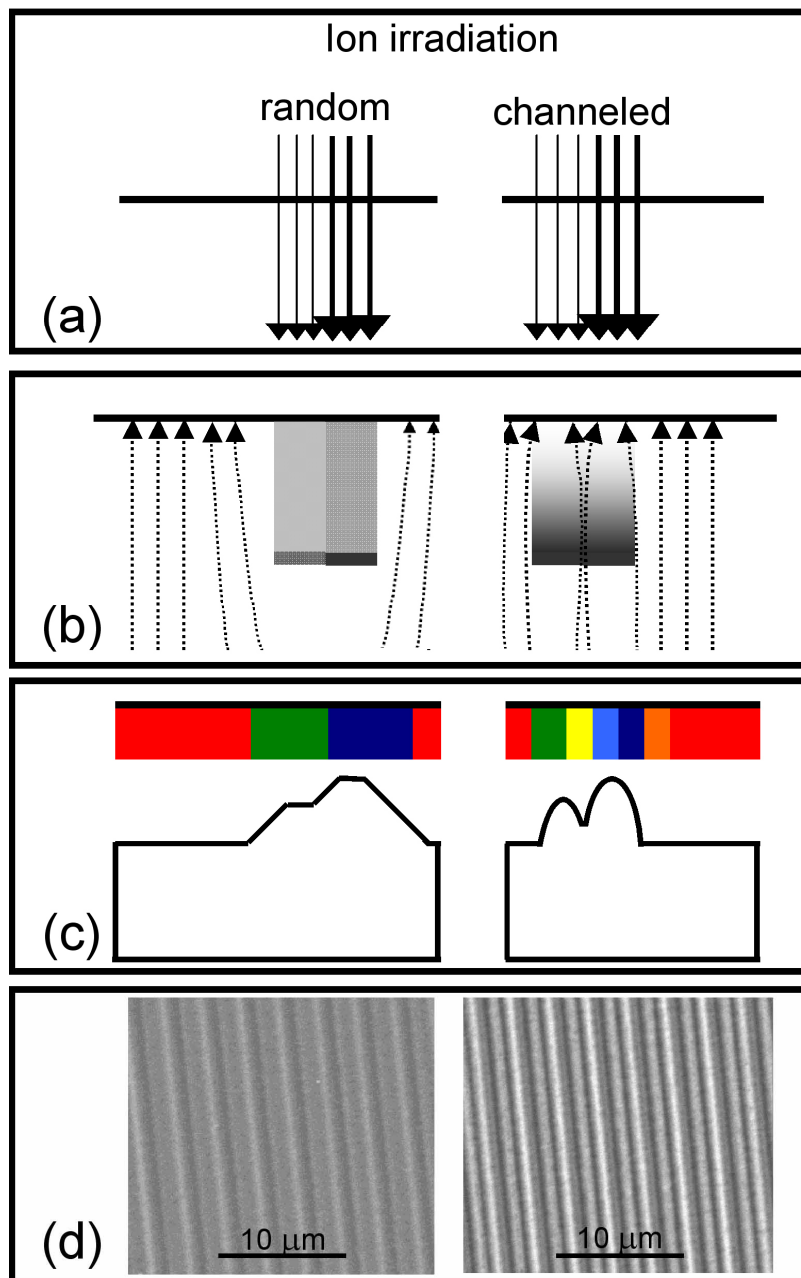


Fig 4. Different effects of channeled and random irradiation. (a) adjacent regions are irradiated with two different doses (lower dose to the left) with the wafer in random and channeled alignment. (b) during anodisation the hole currents flowing through the wafer are deflected round the irradiated regions. (c) shows the silicon surface remaining after anodisation, the Bragg reflecting layers are not shown, only the reflected colour. (d) SEM images of the surfaces of 1  $\mu\text{m}$  wide irradiated lines in (left) random and (right) channeled irradiation.

In a channeled beam irradiation in Fig. 4(a) the defect density close to the surface is reduced by a factor of about five compared with random alignment, rising slowly with increasing depth as the beam dechannels [11, 12]. During anodisation in Fig. 4(b) the hole current is deflected around the end-of-range region but closer to the surface it is bent back towards the irradiated region as a result of its reduced defect density. The lateral width of the anodized features is thus considerably reduced in Fig. 4(c), so the reflected wavelength can be controlled on a smaller lateral scale in channeled compared to random alignment. This is highlighted in Fig. 3(b) which shows a horizontal linescan of the red-green-blue components of the measured reflected light across Fig. 3(a), where the corresponding colour observed is also indicated. As a result of this in Fig. 4(d) it is seen that the irradiated lines in channeled alignment are much narrower than those in random alignment.

Also of note in Fig. 3 is that each irradiated line reflects two colours, with a total of six colours reflected within each 3  $\mu\text{m}$  wide period. Most notable is the presence of a narrow yellow (i.e. red-shifted) line  $\sim 300$  nm in width, between the blue and green irradiated lines. This corresponds to where the porous silicon layers of the Bragg reflector are thicker than both of the blue and green irradiated regions [Fig. 4(c)] and occurs because a small hole current is able to flow through the end-of-range region [Fig. 4(b)] where the defect density is lower than in random irradiation. The lower portion of Fig. 3(a) shows a SEM image of the Bragg reflector produced by channeled irradiation in which the porous silicon has been removed to show the surface profile. The oval profile associated with channeled irradiation for the blue and green irradiated lines is clearly seen, as is the depression between them from which yellow light is reflected. Furthermore, the oval profile associated with each irradiated line in channeled alignment is slightly skewed, being thinner on the side adjacent to a lower dose irradiation where a higher hole current flows. Thus the blue irradiation becomes light blue towards the green irradiation and orange towards the red irradiation.

#### 4. Conclusion

This work provides a means of producing high-density arrays of micron-size reflective colour pixels in the visible spectrum for use in data displays, micro-displays, Liquid Crystal on Silicon (LCOS) and projection televisions. It also demonstrates the possibility of using ion irradiation to selectively tune the wavelengths of porous silicon Fabry-Perot microcavities across both the visible and infra-red ranges for optical communications and computing applications. The pixel size, density and reflectivity demonstrated here are significantly better than that currently attainable with other existing technologies for patterning reflective colour filters. For example, Ocean Optics [17] offer 2  $\mu\text{m}$  wide colour filters with 1  $\mu\text{m}$  wide gaps for transmission purposes, but highly-reflective colour patterning on a micrometer scale has not been previously reported. This fabrication process is also compatible with standard silicon wafer processing involving the use of broad-beam ion irradiation and photolithography to fabricate pixellated regions over entire wafers surfaces for mass production over large areas for displays.